

Towards Robust Sensor Fusion in Visual Perception

Shaojie Wang

Computer Science and Engineering
Washington University in St. Louis
St. Louis, United States
joss@wustl.edu

Tong Wu

Computer Science and Engineering
Washington University in St. Louis
St. Louis, United States
tongwu@wustl.edu

Yevgeniy Vorobeychik

Computer Science and Engineering
Washington University in St. Louis
St. Louis, United States
yvorobeychik@wustl.edu

Abstract—We study the problem of robust sensor fusion in visual perception, especially under the autonomous driving settings. We evaluate the robustness of RGB camera and LiDAR sensor fusion for binary classification and object detection. In this work, we are interested in the behavior of different fusion methods under adversarial attacks on different sensors. We first train both classification and detection models with early fusion and late fusion, then apply different combinations of adversarial attacks on both sensor inputs for evaluation. We also study the effectiveness of adversarial attacks with varying budgets. Experiment results show that while sensor fusion models are generally vulnerable to adversarial attacks, late fusion method is more robust than early fusion. The results also provide insights on further obtaining robust sensor fusion models.

Index Terms—Robust sensor fusion, autonomous driving, adversarial attacks

I. INTRODUCTION

Autonomous driving (AD) depend heavily on visual perception from multiple sensors, such as camera and LiDAR. It is believed that fusion of different sensors provides richer information than a single modality, which further boosts the liability of AD visual perception, e.g., LiDAR point cloud can provide additional depth information for RGB images. Given the stakes in human lives, it is critical to ensure that AD visual perception is robust. Yet, there have been a series of demonstrates that deep neural networks, that provide the core perceptual reasoning machinery, are vulnerable to small adversarial perturbations to inputs [3], [6], [9], [10], [18].

Nevertheless, despite a great deal of research into vulnerability of specific sensors to adversarial examples, there has been little research studying robustness of sensor fusion systems. On the one hand, issue of suboptimal sensor fusion has seen some prior attention, including Movellan and Mineiro [20], who show that performance of fusion models can be worse than single-modality models because the multimodal information is not fused optimally. On the other hand, with the use of deep learning in AD, we also need to pay attention to the robustness of sensor fusion models under adversarial settings.

We propose to investigate three questions related to robust visual sensor fusion in adversarial settings:

- 1) Is the fusion model robust against adversarial attacks on one or more sensors?
- 2) Which fusion paradigms, early or late fusion, are more robust?

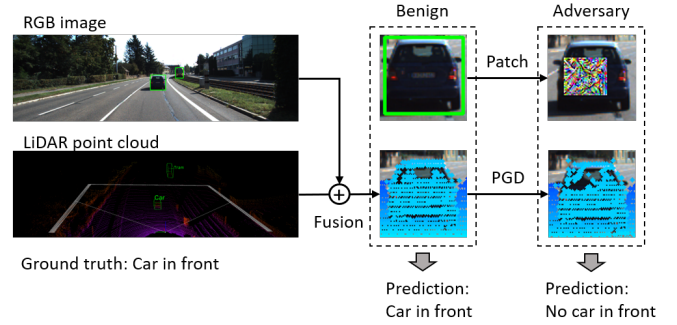


Fig. 1: An example of adversarial attack on sensor fusion (early) model. We apply adversarial patch on the RGB image, and PGD attack on the original 3D point cloud which causes point shifting on the depth map. Note that in our model, we are taking the entire RGB-D image as input. The cropped car is for illustration only.

- 3) How can we develop robust fusion models against adversarial attacks?

Yu et al. [41] recently partially explored the first question. They study the vulnerability of a particular sensor fusion approach under different sensor attacks, while we are also interested in behaviors of fusion models under other circumstances, e.g., when one of the input sensors is disabled.

To answer these questions, we focus on evaluating the robustness of sensor fusion in visual perception from RGB camera and LiDAR. To simplify the problem, we focus on detecting whether there is car in front or not, to mimic the real world scenario where we want to make decisions about whether to brake. We study both classification and detection tasks under this setting. For classification tasks, we train models to make binary decisions, while in detection, we keep the normal routine of detection models, and decide whether there is car in front using the predicted bounding boxes.

For the first question, we apply projected gradient descent (PGD) attacks [19] with l_p -norm restrictions on both camera and LiDAR sensors for all models. The attack on camera image is restricted to a patch within the car bounding box, to simulate the situation where the car surface is partially covered. For LiDAR attack, we restrict the perturbation to points within the car bounding box. For ablation study, we also apply LiDAR attack on the entire point cloud and on the

background points. Then, we study the effectiveness of attacks under different budgets: for the LiDAR attack, we vary the ϵ bound on the l_p -norm restriction, while for the image attack we vary the size of the adversarial patch.

For the second question, we compare two widely used fusion methods, early fusion and late fusion. For early fusion, we project 3D LiDAR points onto the RGB image pixels as the depth map. For late fusion, we concatenate the convolutional features of RGB image and LiDAR point cloud for the final prediction. In Fig. 1, we illustrate an example of adversarial attacks on camera and LiDAR sensors in early fusion models. Through the experiments, we will discuss the possible solutions to the third problem and the potential difficulties in achieving robust sensor fusion.

The rest of the paper are organized as follows. In section II, we sum up the related works. Section III introduces the baseline models, fusion strategy, and attack methods used in this work. In section IV, we have experiment setups, results, and discussion on robust sensor fusion. Conclusions are drawn in section V.

II. RELATED WORKS

A. Robust sensor fusion

Sensor fusion, or multimodality, has been a widely studied topic with the rise of deep learning. Data collected from multiple sensors are fused together to deal with complex tasks, e.g., audio-visual fusion in speech recognition (e.g. [8], [21]) and video captioning (e.g. [27], [36]).

In autonomous driving (AD), fusion of LiDAR point clouds and RGB images are very frequently used. Depending on different stages of fusion, we can divide sensor fusion into early fusion and late fusion. Some literature, e.g. [11], has an additional class called middle fusion. In our paper, late fusion refers to fusion happening after all the convolutional layers. The detailed definition is in section III. Most early fusion models uses RGB-D images as input where LiDAR points are converted into depth map as an additional channel for RGB images, e.g. MVX-Net [32], AVOD [14], Frustum PointNet [25]. Some other early fusion methods project RGB images onto bird-eye view (BEV) plane of LiDAR point clouds (e.g. [38]). The idea behind different early fusion methods is the same, which is to align both sensors in the same representation space and extract joint features. The simplest late fusion method is naive feature concatenation (e.g. [24]). In object detection, late fusion can also happen after region proposals (e.g. [1]). Multi-stage fusion is also widely used (e.g. [16]). In our work, we specify early fusion as RGB-D, and late fusion as naive feature concatenation. Other sensors like radar [5], thermal image [17] and HD-map [40] are also used in AD sensor fusion. We refer the readers to [11] for a much more detailed literature review on AD sensor fusion.

As for robust sensor fusion, [20] studies the robustness of audio-visual fusion against catastrophic fusion problem in speech recognition. [42] proposes a multimodal model which is robust to the absence of some sensors. [31] focuses on the uncertainty of input data from different sensors, including

the differences in physical units of measurement, sampling resolutions, and spatio-temporal alignment. However, there is no previous work on robustness of sensor fusion models against adversarial attacks, which is a raising concern with the use of deep learning.

B. Adversarial perturbations

We focus on literature about adversarial perturbations on visual perception using RGB camera and LiDAR sensors.

1) *RGB Image*: In the literature of adversarial attack on images [13], [15], [19], [22], [35], [37], white-box attacks and black-box attacks are the two main categories. In white-box attacks, attackers have access to all the information of the model, while in black-box attacks, the information of the model is partially or entirely concealed. In our work, we assume that the attackers have white-box access to the models, and that they use projected Gradient Descent (PGD) [19] which is a considerably stronger white-box attacks. There are also works on black-box attacks on traffic signs, e.g., [23].

Image attack is also the most studied topic in adversarial perturbation on AD because of its low cost and rich literature. Most AD related adversarial attacks target on traffic signs, e.g. [9] proposes a physically realizable attack on traffic sign classifier, and [6], [10], [18] generate malicious signs to fool object detectors. There are also attacks trying to confuse the decision system of AD. [7] proposes an evasion attack against the steering angle prediction which causes the autonomous car to head towards wrong directions.

Adversarial patch [2], originally proposed to attack image classifiers, are also applied on AD related systems. [28] put a patch in video to attack optical flow. [33] attaches adversarial patch on a person to make them invisible to YOLOv2 object detector. In our work, we follow the objective in [33] to attack YOLOv3 detector, while the target is car instead of person.

2) *LiDAR*: In [39], they perturb the entire point cloud with no restrictions. However, this attack is not physically realizable because it is not easy to arbitrarily add or shift LiDAR points. [3] uses sensor spoofing to add adversarial points into the point cloud read by the LiDAR sensor to attack the machine learning model in LiDAR-based perception. Other physically realizable attacks uses real-world objects to fool the models, e.g., [4] designs an adversarial object which cannot be detected by LiDAR-based perceptions, and [34] attaches adversarial mesh over the roof of the car to attack LiDAR detectors.

3) *Fusion*: [41] is a very recent and the only paper to our knowledge that studies adversarial attacks on fusion models. They claim that current fusion models fail to use the complementary relationships among different sensors in the adversarial setting. In our work, we not only evaluate different sensor attacks on fusion models, but also compare the attacks with disabled sensors, i.e. no input from those sensors, to evaluate the contribution of each sensor to the prediction. Moreover, we study the effect of different fusion methods on adversarial attacks, while they only use early fusion model for evaluation.

III. MODELS

In this section, we introduce the models and the attack methods we use for the evaluation.

A. Baseline models

We can formulate a deep sensor fusion model with n sensors as

$$y = f(\mathbf{x}_1, \mathbf{x}_2, \dots, \mathbf{x}_n; \theta), \quad (1)$$

where f is the neural network model, \mathbf{x}_i stands for the i -th sensor input, θ for the neural network parameters, and y is the output of the model, which can be interpreted as class label for classification, or bounding box prediction for detection. In this work, we focus on fusion of two sensors, i.e. RGB camera and LiDAR.

Before going further into any details, we first define early fusion and late fusion used in our paper. In early fusion, two sensors are fused at the input level. For image and LiDAR, we convert LiDAR into depth map, and add it as an additional channel to the RGB image. In late fusion, we use feature concatenation after the feature extractor of each model.

1) *Classification*: We use VGG16 and ResNet18 for the image classifier, and PointNet [26] for the LiDAR classifier. For simplicity, we use ConvNet to refer to both VGG and ResNet. Late fusion of classification concatenates the convolutional features of ConvNet and PointNet, then feed the fused feature to a new set of fully connected layers for further training, as shown in Fig. 2a. Fig. 2b illustrates early fusion model using RGB-D image as input to ConvNet. In detail, LiDAR points are projected onto the RGB image pixel space as an additional depth channel, and a fifth channel is attached to indicate the non-zero values of the depth channel using 0's and 1's. We use a differentiable RGB-D module implemented via kornia [30] to generate RGB-D images out of RGB images and LiDAR points, so that the adversarial perturbation can be applied directly on the 3D point cloud instead of on the depth map.

2) *Detection*: Detection task is more complex than classification. Some detection models such as the RCNN family use a two-stage structure (region proposal and object classification), while YOLO only needs one stage (generating proposals and classification results at the same time). For two-stage detection models, it is ambiguous whether feature concatenation in region proposal networks should be called late fusion or early fusion. To make the concepts clear, we use the single-stage YOLOv3 [29] as the detection model. The structures of both late fusion and early fusion models are similar to classification which are already shown in Fig. 2. The only difference lays in the late fusion model, where YOLOv3 has shortcut connections between Darknet, the feature extractor, and the YOLO layers. In our work, we simply concatenate the LiDAR feature with RGB image feature after the Darknet. The intermediate features are not fused, meaning that the shortcuts only pass RGB image features to the YOLO layers.

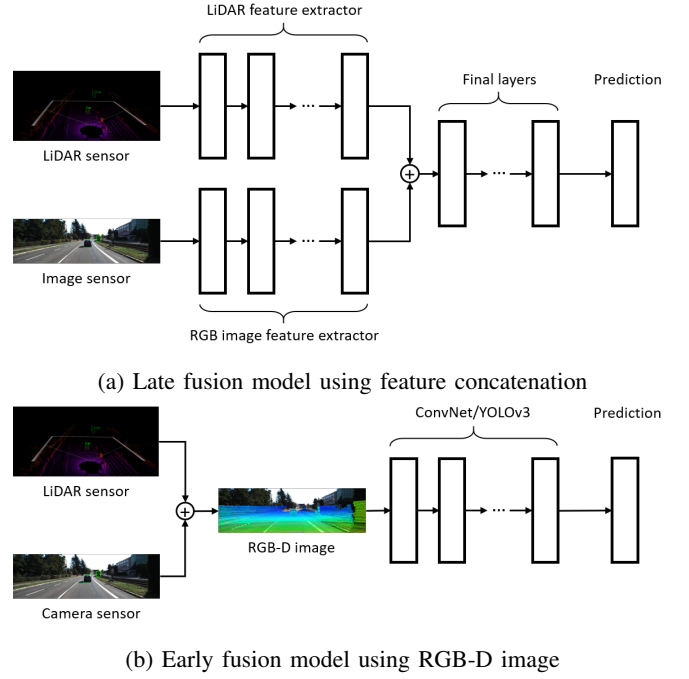


Fig. 2: Structure of late fusion and early fusion models. “ \oplus ” stands for the fusion operation. In (a), the LiDAR feature extractor is the convolutional layers in PointNet for classification, and Darknet for detection. Note that in classification, PointNet feature extractor takes the original point cloud as input, while in detection, Darknet takes depth map as input. Similarly, the RGB image feature extractor is the convolutional layers in ConvNet for classification, and Darknet for detection. The final layers are fully connected layers for classification, and YOLO layers for detection.

B. Threat models

In this work, we study the effect of adversarial attacks on both classification and detection models. Commonly, the problem of attacking one or more sensors in a sensor fusion model can be formulated as

$$\begin{aligned} \arg \max_{\delta} L(f(\dots, \mathbf{x}_i + \mathbf{m}_i * \delta_i, \dots; \theta), y) \\ \text{s.t. } \mathbf{m}_i \in \mathbf{M}, \\ \|\delta_i\|_p \leq \epsilon_i, \forall i \in \mathcal{I}, \\ \delta_i = 0, \forall i \in \mathcal{I}^c, \end{aligned} \quad (2)$$

where $L(\cdot)$ is the attacker’s utility function, \mathbf{x}_i is the i -th sensor input, δ_i is the perturbation, ϵ_i is the l_p -norm restriction, \mathcal{I} stands for the set of sensors to be attacked, \mathcal{I}^c for the set of sensors remaining normal, and \mathbf{m} denotes the projection restriction inside the feasible region \mathbf{M} , which can be the car bounding box, the entire image, or the entire point cloud depending on which sensor is attacked and what level of restriction is applied. Note that we have different ϵ ’s for different sensors attacked, because different sensors have different measurement of scale in their original input space,

e.g. in RGB image, l_p norm shows the pixel difference, while in LiDAR point cloud, l_p norm means the physical world distance.

Adversarial attacks on image branch is rather easy, as there are many previous works such as adversarial stickers. We leverage adversarial stickers computed via projected gradient descent (PGD), to partially cover the surface of cars. To achieve this goal, we place the sticker within the 2D bounding box of cars, and use grid search to find the best initialization location of the sticker.

For LiDAR attacks, we focus on PGD attacks with l_p -norm restriction, which is a simple but reasonable way to study the robustness of fusion models. The attack will only shift points in the 3D space. Adding or removing points are not allowed. We try attacks within the 3D bounding boxes of cars, as well as on the entire point cloud and the background points respectively to study what the LiDAR model has learned from the input data. For models using RGB-D feature, the PGD attack is still posed to the original point cloud instead of the depth map.

The attack objective for classification is to make the model fail to predict cars in front. The utility function L is the cross entropy loss, targeted at the positive class, namely “car in front”. For attacks on detection models, we aim to make the model detect nothing in front even if there is a car. The attack fails when the IoU between the predicted bounding box and the ground truth bounding box is greater than 0.1. We use the similar loss function, objectness score of the front car, proposed in [33] to generate adversarial perturbations on YOLOv3 model.

IV. EXPERIMENT RESULTS

We perform the experiments on KITTI [12] dataset. The dataset has 7,481 samples with 2D and 3D bounding box provided. The LiDAR coordinate system in KITTI dataset is defined as: $+x$ means front, $+y$ is left, and $+z$ points upward. We define the front region as

$$F = \{p(x_p, y_p, z_p) | x_p \in [0, 20], y_p \in [-1.8, 1.8]\},$$

i.e. the area 20 meters ahead within the current lane (usually a lane in the US is about 3.6 meters wide). There is no constraint on z_p because all cars are on the surface of the road. A car is in front if the 3D bounding box of the car overlaps with F .

TABLE I: Accuracy scores of individual models

Models	Original Accuracy
Image (VGG)	0.977
Image (ResNet)	0.969
LiDAR	0.894
Late fusion (VGG)	0.977
Late fusion (ResNet)	0.970
Early fusion (VGG)	0.992
Early fusion (ResNet)	0.977

A. Classification

In the experiments, we are measuring the **attack success rate** on “car-in-front” class. We choose a subset of KITTI

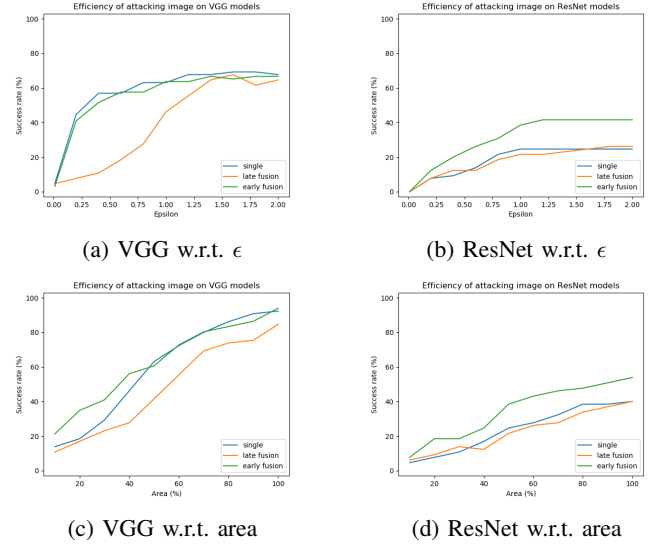


Fig. 3: Comparison of image attacks on single-image, early fusion, and late fusion models. ϵ is the l_∞ budget of the PGD attack, and area is the ratio of patch size and the bounding box size.

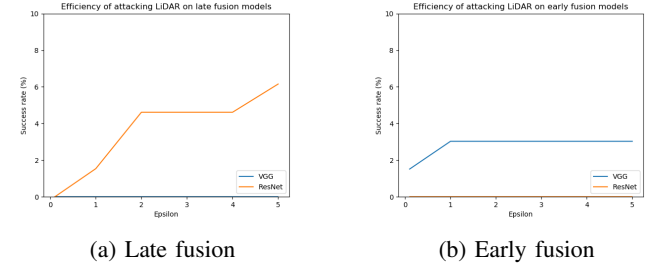


Fig. 4: l_∞ LiDAR attack on the entire point cloud w.r.t. different ϵ on early and late fusion models. Y-axis is scaled within 0 – 10%.

dataset to perform the binary classification task. Samples of “car in front” class are selected by the overlapping rule mentioned above, and there are 219 such samples in the entire dataset. Samples of “no car” class are selected if no car bounding boxes overlaps with $\{p | x_p \in [0, 40], y_p \in [-3.6, 3.6]\}$, a larger region in front. This is to avoid ambiguous situations where a car lies on the edge of region F . To ensure the class distribution is balanced, we further randomly select samples from this subset. Eventually, we have 306 samples for training and 132 samples for validation, and the class distribution is 50 to 50 in both sets.

We first train all the models needed for ablation studies in adversarial attacks. The results are shown in Table I. Then, in Fig. 3, we plot the success rate of image attack on different models with respect to different ϵ ’s and patch sizes. E.g. in Fig. 3a, we illustrate how the attack success rate changes with different ϵ ’s among late fusion, early fusion, and single models using VGG as backbone. From all 4 subfigures, we can see that

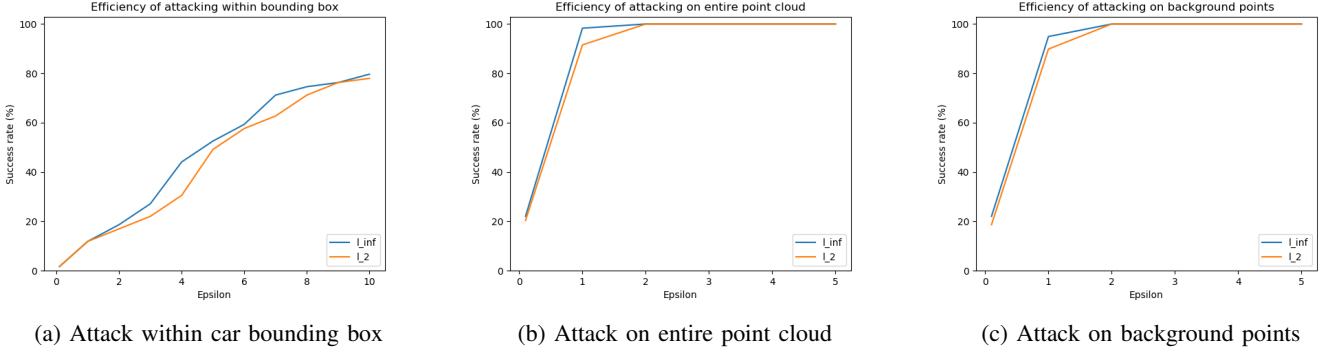


Fig. 5: LiDAR attack effect w.r.t. different ϵ on PointNet.

early fusion models are as vulnerable as single image models when using VGG as backbone, and are more vulnerable than single models when using ResNet as backbone. On the contrary, late fusion models are less vulnerable, as we can see the obvious gap between the two fusion methods. Moreover, we can see that although fusion models with VGG backbone and ResNet backbone have similar accuracy scores, models with VGG backbone are more vulnerable than models with ResNet backbone.

Attacking LiDAR is not effective on fusion models. If we restrict the perturbation to points within the car bounding boxes, the success rates are always 0 under various ϵ 's. Therefore, in Fig. 4, we show the results of adversarial attack on the entire point cloud, which contain nonzero values to plot meaningful figures. We can see that the success rate of l_{∞} attack on LiDAR is very low on both late and early fusion models, even with a fairly large ϵ . If we try l_2 restriction, the success rates also drop to 0. One possibly reason is that the LiDAR model is effectively ignored in the fused models. However, accuracy of fusion models is higher than when we use image-only models, suggesting that LiDAR does indeed play some role in prediction.

To demonstrate that the failure of attacks on LiDAR in the fusion models is not due to the failure of our algorithm, we analyze the adversarial attack on single LiDAR model, i.e. PointNet. In Fig. 5b, we can see that PointNet is extremely vulnerable to adversarial attacks even when $\epsilon = 1$. Even if we only perturb the points within the car bounding boxes, we can still achieve higher success rate on PointNet than on fusion models. The interesting thing is that attacking the background points, as shown in Fig. 5c is almost as effective as attacking the entire point cloud. This means that the classification task on point cloud is not only learning the car itself, but the entire environment (for example, absence of points in the area where the car is may also be highly informative). In any case, this provides additional evidence that sensor fusion may significantly reduce the vulnerability of LiDAR-based perception, whereas attacks on the image branch of the fusion model remain highly effective.

Apart from image and LiDAR attacks, we also consider disabling either sensors, i.e. cancelling out either image or

LiDAR input as a type of attack, since it also causes misclassification, to have reasonable comparisons among different combinations of attacks. For early fusion, we simply set the channel to be cancelled in RGB-D images to zero, e.g., if we disable the LiDAR sensor, we manually set the values of depth and indicator matrices to 0. For late fusion, we manually set the feature vector of disabled sensor to 0 during concatenation.

In table II, we evaluate different combinations of attacks with fixed ϵ for both attacks ($\epsilon_{image} = 1, \epsilon_{lidar} = 5$) and fixed patch size for image attacks ($area = 50\%$). Because LiDAR attack within car bounding boxes has no effect on all the fusion models, we report the results of attacks on the entire point cloud to have a meaningful comparison. In column 1, the success rate of LiDAR attack is extremely low. From columns 3 and 4, we can see that the image branch dominates the prediction in both fusion models. The joint attack of image and LiDAR has lower success rate than image attack only as listed in columns 2 and 5, which implies that under the same restrictions, simply optimizing the objective in Eq. 2 might not be optimal when it comes to multiple sensors. An interesting phenomenon observed from columns 2 and 6 is that the image attack on early fusion models is less effective when the LiDAR sensor is disabled.

It is also interesting to notice from columns 4, 8, and 9 that cancelling image channel causes late fusion models to predict everything as “car in front” class, but disabling the sensor literally means the prediction should be “no car” based on its input. The possible reason is that in the feature concatenation layer, the bias term is not modified even when both sensors are disabled, and the last few layers of the model uses information from the bias term to make false predictions.

As an attempt to circumvent this issue, we use feature dropout to retrain the fusion models. The idea is that sensor fusion models should be robust against the absence of part of the sensors. During training, we randomly replace either image or LiDAR feature with zeros, and the results on models trained with feature dropout are shown in table III and IV. We can see from column 4 in table IV that ResNet late fusion model and VGG early fusion model has better performance when we disable the camera sensor. However, this brings us lower overall accuracy, and the vulnerability issue remains unsolved.

TABLE II: Evaluation of attacks on fusion models. LiDAR attacks are l_∞ attacks on entire point cloud. ✓ means true data, ✗ means adversarial data, \mathcal{N} means disabled sensor. * denotes that although the success rate on “car in front” class is 0, the success rate on “no car” class is 1.0.

Image	✓	✗	✓	\mathcal{N}	✗	✗	\mathcal{N}	\mathcal{N}
LiDAR	✗	✓	\mathcal{N}	✓	✗	\mathcal{N}	✗	\mathcal{N}
success rate (late VGG)	0.0	0.446	0.0	0.0*	0.431	0.492	0.0*	0.0*
success rate (late ResNet)	0.062	0.215	0.077	0.0*	0.215	0.354	0.0*	0.0*
success rate (early VGG)	0.030	0.636	0.030	0.985	0.530	0.484	1.0	1.0
success rate (early ResNet)	0.0	0.385	0.0	1.0	0.354	0.215	1.0	1.0

TABLE III: Accuracy of models trained with feature dropout

Models	Original Accuracy
Late fusion (VGG)	0.977
Late fusion (ResNet)	0.954
Early fusion (VGG)	0.977
Early fusion (ResNet)	0.939

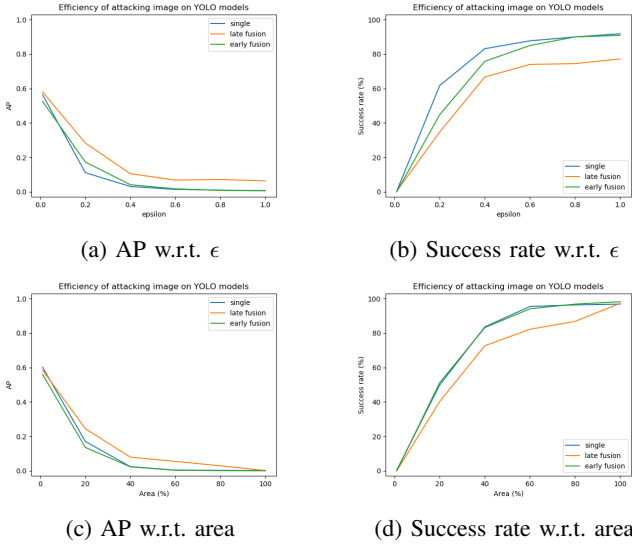


Fig. 6: Comparison of image attacks on different detection methods. ϵ is the l_∞ budget of the PGD attack, and area is the ratio of patch size and the bounding box size.

B. Detection

In detection, we train and validate the fusion models on the entire KITTI dataset. The measurement of attack success rate on detection models is slightly different. We still focus on the “car in front” samples in the test set (66 in total which are not used when the detection models are trained), but the objective is to reduce the objectness score, i.e. to make the car undetected rather than to cause misclassification. We say the attack is successful if the IoU of the predicted car bounding box and the ground truth label is less than 0.1. We also report the average precision (AP) of the car detection. The ϵ ’s and patch size used for table V are also the same as classification.

Similar to classification, we show how the AP and success rate of image attack on detection models change with different ϵ ’s and patch sizes in Fig. 6. We can see that most conclusions obtained on classification models also apply to detection

models. Late fusion in detection is more robust than both early fusion and single model. Also, we can see that AP the detection models can nearly drop to 0 with larger ϵ or patch size, and that in terms of attack success rate, using detection models are more vulnerable than using classification models.

Also similar to classification, LiDAR attack does not affect the performance of detection models much. The success rate of LiDAR attack on both late and early fusion models are 0, while the AP of early fusion drops 0.002 under the LiDAR attack. However, when we look at column 4 in table V, we can see a significant drop in AP when we disable the camera sensor, even though the success rate is still 0. When comparing columns 3 and 5, we find that disabling camera in late fusion model will cause a strange phenomenon where the success rate is 0 but the AP is very low. We further investigate the detection model and find that after we disable the camera sensor, the model predicts 10 times as many bounding boxes than the normal model does. Similar situation occurs in the corresponding experiment of the last column. This might be the inherent flaw of YOLO models which is out of the scope of our discussion. As shown in columns 3 and 6, the joint attack of both sensors is still less effective on early fusion models than the image attack, as it has slightly lower success rate and higher AP after the attack.

C. Discussion

From the experiments on both classification and detection models, we can go back to the three questions we proposed:

1) *Is fusion model robust against adversarial attacks on one or more sensors?*: The answer is yes. We obtain similar results with the concurrent work in [41], that the fusion models are still vulnerable to adversarial attacks. Their work did not compare the contribution of each sensor in the fusion model.

2) *Will different fusion methods affect the effectiveness of adversarial attacks?*: The answer is also yes. We have observed that late fusion models are more robust than early fusion models under the same amount of attack for both classification and detection tasks. The structure of early fusion model, when compared with late fusion model, is obviously more similar to the single image model. Therefore, the curves of early fusion models are closer to those of single models. For late fusion models, even though attacking the LiDAR branch does not affect the overall performance, the effectiveness of image attack is limited.

3) *How can we build robust fusion models against adversarial attacks?*: Our work provides some insights on this

TABLE IV: Evaluation of attacks on fusion model (trained with dropout). LiDAR attacks are l_∞ attacks on entire point cloud. ✓ means true data, ✗ means adversarial data, \mathcal{N} means disabled sensor. The numbers in () shows the success rate on “no-car” class if greater than 0. Note that this is only effective with disabled sensors.

Image	✓	✗	✓	\mathcal{N}	✗	✗	\mathcal{N}	\mathcal{N}
LiDAR	✗	✓	\mathcal{N}	✓	✗	\mathcal{N}	✗	\mathcal{N}
success rate (late VGG)	0.0	0.615	0.0	0.0 (1.0)	0.6	0.631	0.0 (1.0)	0.0 (1.0)
success rate (late ResNet)	0.0	0.2	0.0	0.292 (0.328)	0.2	0.169	0.352 (0.328)	0.0 (1.0)
success rate (early VGG)	0.0	0.563	0.0 (0.015)	0.328 (0.215)	0.5	0.438 (0.015)	0.047 (0.215)	1.0
success rate (early ResNet)	0.016	0.222	0.032 (0.016)	0.032 (0.918)	0.206	0.222 (0.016)	0.0 (0.918)	1.0

TABLE V: Evaluation of attacks on detection models. LiDAR attacks are l_∞ attacks on entire point cloud.

Image	✓	✓	✗	✓	\mathcal{N}	✗	✗	\mathcal{N}	\mathcal{N}
LiDAR	✓	✗	✓	\mathcal{N}	✓	✗	\mathcal{N}	✗	\mathcal{N}
Late fusion	success rate	0.0	0.0	0.749	0.0	0.0	0.754	0.712	0.0
	AP	0.603	0.603	0.068	0.345	0.055	0.064	0.043	0.055
Early fusion	success rate	0.0	0.0	0.922	0.0	1.0	0.918	0.932	1.0
	AP	0.607	0.605	0.005	0.606	0.0	0.006	0.004	0.0

question. First of all, the comparison of early and late fusion methods tells us that although early fusion models have higher accuracy or average precision scores than late fusion models, late fusion can make the model more robust than early fusion. Second, in Fig. 3, by comparing the VGG backbone models and ResNet backbone models from the classification experiments set, we observe that ResNet is more robust than VGG against image attacks, so does the fusion models using ResNet as backbone when compared to those using VGG. We may assume that the robustness of the backbone models can contribute to the robustness of fusion models, so we can train robust single-sensor models before training the fusion models. Still, more experiments are needed to validate this assumption. Third, existing methods of building robust sensor fusion may not work under adversarial settings. Feature dropout as the simplest way of gaining robustness against disabled sensors is applied on classification models, yet the effect is subtle, as it only partially circumvent the issue for some models. What is worse, it makes the fusion model more vulnerable to adversarial perturbations. The method proposed in [42] is robust to the absence of some sensors, but they are using deep neural networks as the model, which might still be vulnerable to adversarial attacks. More evaluations in adversarial settings are needed for these sensor fusion methods.

All the experiments are based on the binary decision of detecting whether there is car in front or not, while the mechanisms behind this decision, e.g. classification and detection, may or may not be binary. We already discuss the situations with static scenes provided by the KITTI dataset. When faced with dynamic decisions where we need to adjust to the change of environments across a sequence of sensor snapshots, the task could be more complex. Meanwhile, our work can still be a valuable reference. In general, a more complex system is more vulnerable and easier to attack. When we use detection models for the binary decision, we first generate the bounding boxes and class labels, then we decide whether the car is in front or not. This gives us more freedom during attacks than in classification tasks, especially binary classification. In a more complex system involving dynamic scenes, the vulnerability

of the model will increase.

Nevertheless, this work has set the tone of studying the adversarial robustness of fusion models. Not only do we need to study the trend of attack effectiveness with various budgets, but we also need to evaluate the contribution of each sensor to the overall performance and robustness of the fusion model, e.g. comparing adversarial attacks with disabling sensors, and different combinations of them. Moreover, there are many more complicated fusion methods such as the mixture of late and early fusion where the fusion happens at multiple places during the forward passing, and robust fusion methods resolving the issue of disabled sensors, but are still potentially vulnerable to adversarial attacks. Also, there are still questions not answered such as “Can adversarial attack on one sensor infiltrate other sensors?”, which will be left as future work.

In the experiments, we have some other interesting observations. If we attack the two sensors independently, the success rate will be even lower than jointly attacking both sensors, which is already inferior to attacking a single sensor. Note that the upper bound of l_p -norm restriction is different across different sensors, e.g. image perturbation is limited by the range of valid pixel values, and LiDAR points can be shifted arbitrarily away if we do not consider the limit LiDAR scan range or the realizability of the attack in physical world settings. How to optimally attack multiple sensors at the same time is also a possible future work direction.

V. CONCLUSION

This work focuses on the robustness of sensor fusion models in visual perception using RGB camera and LiDAR. We evaluate two different fusion methods, early fusion and late fusion, in a simplified environment where we want to make a binary decision on whether there is car in front or not. Both classification and detection are studied in the experiments, and the behavior of both tasks are similar and consistent. We find that both fusion methods are vulnerable to adversarial attacks, but late fusion is relatively more robust than early fusion. We set the tone of studying adversarial robustness on fusion

models, which provides grist for the mill for designing robust sensor fusion models.

REFERENCES

- [1] A. Asvadi, L. Garrote, C. Prenebida, P. Peixoto, and U. J. C. Nunes. Multimodal vehicle detection: fusing 3d-lidar and color camera data. *Pattern Recognit. Lett.*, 115:20–29, 2018.
- [2] T. B. Brown, D. Mané, A. Roy, M. Abadi, and J. Gilmer. Adversarial patch. *CoRR*, abs/1712.09665, 2017.
- [3] Y. Cao, C. Xiao, B. Cyr, Y. Zhou, W. Park, S. Rampazzi, Q. A. Chen, K. Fu, and Z. M. Mao. Adversarial sensor attack on lidar-based perception in autonomous driving. In L. Cavallaro, J. Kinder, X. Wang, and J. Katz, editors, *Proceedings of the 2019 ACM SIGSAC Conference on Computer and Communications Security, CCS 2019, London, UK, November 11-15, 2019*, pages 2267–2281. ACM, 2019.
- [4] Y. Cao, C. Xiao, D. Yang, J. Fang, R. Yang, M. Liu, and B. Li. Adversarial objects against lidar-based autonomous driving systems. *CoRR*, abs/1907.05418, 2019.
- [5] S. Chadwick, W. Maddern, and P. Newman. Distant vehicle detection using radar and vision. In *International Conference on Robotics and Automation, ICRA 2019, Montreal, QC, Canada, May 20-24, 2019*, pages 8311–8317. IEEE, 2019.
- [6] S. Chen, C. Cornelius, J. Martin, and D. H. P. Chau. Shapeshifter: Robust physical adversarial attack on faster R-CNN object detector. In M. Berlingerio, F. Bonchi, T. Gärtner, N. Hurley, and G. Ifrim, editors, *Machine Learning and Knowledge Discovery in Databases - European Conference, ECML PKDD 2018, Dublin, Ireland, September 10-14, 2018, Proceedings, Part I*, volume 11051 of *Lecture Notes in Computer Science*, pages 52–68. Springer, 2018.
- [7] A. Chernikova, A. Oprea, C. Nita-Rotaru, and B. Kim. Are self-driving cars secure? evasion attacks against deep neural networks for steering angle prediction. In *2019 IEEE Security and Privacy Workshops, SP Workshops 2019, San Francisco, CA, USA, May 19-23, 2019*, pages 132–137. IEEE, 2019.
- [8] S. Dupont and J. Luetttin. Audio-visual speech modeling for continuous speech recognition. *IEEE Trans. Multimedia*, 2(3):141–151, 2000.
- [9] K. Eykholt, I. Evtimov, E. Fernandes, B. Li, A. Rahmati, C. Xiao, A. Prakash, T. Kohno, and D. Song. Robust physical-world attacks on deep learning visual classification. In *2018 IEEE Conference on Computer Vision and Pattern Recognition, CVPR 2018, Salt Lake City, UT, USA, June 18-22, 2018*, pages 1625–1634. IEEE Computer Society, 2018.
- [10] K. Eykholt, I. Evtimov, E. Fernandes, B. Li, D. Song, T. Kohno, A. Rahmati, A. Prakash, and F. Tramèr. Note on attacking object detectors with adversarial stickers. *CoRR*, abs/1712.08062, 2017.
- [11] D. Feng, C. Haase-Schuetz, L. Rosenbaum, H. Hertlein, F. Timm, C. Glaeser, W. Wiesbeck, and K. Dietmayer. Deep multi-modal object detection and semantic segmentation for autonomous driving: Datasets, methods, and challenges. *arXiv:1902.07830*, 2019.
- [12] A. Geiger, P. Lenz, C. Stiller, and R. Urtasun. Vision meets robotics: The kitti dataset. *International Journal of Robotics Research (IJRR)*, 2013.
- [13] I. J. Goodfellow, J. Shlens, and C. Szegedy. Explaining and harnessing adversarial examples. In Y. Bengio and Y. LeCun, editors, *3rd International Conference on Learning Representations, ICLR 2015, San Diego, CA, USA, May 7-9, 2015, Conference Track Proceedings*, 2015.
- [14] J. Ku, M. Mozifian, J. Lee, A. Harakeh, and S. L. Waslander. Joint 3d proposal generation and object detection from view aggregation. In *2018 IEEE/RSJ International Conference on Intelligent Robots and Systems, IROS 2018, Madrid, Spain, October 1-5, 2018*, pages 1–8. IEEE, 2018.
- [15] Y. Li, H. Zhang, C. Bermudez, Y. Chen, B. A. Landman, and Y. Vorobeychik. Anatomical context protects deep learning from adversarial perturbations in medical imaging. *Neurocomputing*, pages 370–378, 2020.
- [16] M. Liang, B. Yang, S. Wang, and R. Urtasun. Deep continuous fusion for multi-sensor 3d object detection. In V. Ferrari, M. Hebert, C. Sminchisescu, and Y. Weiss, editors, *Computer Vision - ECCV 2018 - 15th European Conference, Munich, Germany, September 8-14, 2018, Proceedings, Part XVI*, volume 11220 of *Lecture Notes in Computer Science*, pages 663–678. Springer, 2018.
- [17] J. Liu, S. Zhang, S. Wang, and D. N. Metaxas. Multispectral deep neural networks for pedestrian detection. In R. C. Wilson, E. R. Hancock, and W. A. P. Smith, editors, *Proceedings of the British Machine Vision Conference 2016, BMVC 2016, York, UK, September 19-22, 2016*. BMVA Press, 2016.
- [18] J. Lu, H. Sibai, E. Fabry, and D. A. Forsyth. NO need to worry about adversarial examples in object detection in autonomous vehicles. *CoRR*, abs/1707.03501, 2017.
- [19] A. Madry, A. Makelov, L. Schmidt, D. Tsipras, and A. Vladu. Towards deep learning models resistant to adversarial attacks. In *6th International Conference on Learning Representations, ICLR 2018, Vancouver, BC, Canada, April 30 - May 3, 2018, Conference Track Proceedings*. OpenReview.net, 2018.
- [20] J. R. Movellan and P. Mineiro. Robust sensor fusion: Analysis and application to audio visual speech recognition. *Mach. Learn.*, 32(2):85–100, 1998.
- [21] Y. Mroueh, E. Marcheret, and V. Goel. Deep multimodal learning for audio-visual speech recognition. In *2015 IEEE International Conference on Acoustics, Speech and Signal Processing, ICASSP 2015, South Brisbane, Queensland, Australia, April 19-24, 2015*, pages 2130–2134. IEEE, 2015.
- [22] R. Pang, H. Shen, X. Zhang, S. Ji, Y. Vorobeychik, X. Luo, A. X. Liu, and T. Wang. A tale of evil twins: Adversarial inputs versus poisoned models. In *ACM Conference on Computer and Communication Security*, 2020.
- [23] N. Papernot, P. D. McDaniel, I. J. Goodfellow, S. Jha, Z. B. Celik, and A. Swami. Practical black-box attacks against machine learning. In R. Karri, O. Sinanoglu, A. Sadeghi, and X. Yi, editors, *Proceedings of the 2017 ACM on Asia Conference on Computer and Communications Security, AsiaCCS 2017, Abu Dhabi, United Arab Emirates, April 2-6, 2017*, pages 506–519. ACM, 2017.
- [24] A. Pfeuffer and K. Dietmayer. Optimal sensor data fusion architecture for object detection in adverse weather conditions. In *21st International Conference on Information Fusion, FUSION 2018, Cambridge, UK, July 10-13, 2018*, pages 1–8. IEEE, 2018.
- [25] C. R. Qi, W. Liu, C. Wu, H. Su, and L. J. Guibas. Frustum pointnets for 3d object detection from RGB-D data. In *2018 IEEE Conference on Computer Vision and Pattern Recognition, CVPR 2018, Salt Lake City, UT, USA, June 18-22, 2018*, pages 918–927. IEEE Computer Society, 2018.
- [26] C. R. Qi, H. Su, K. Mo, and L. J. Guibas. Pointnet: Deep learning on point sets for 3d classification and segmentation. *CoRR*, abs/1612.00593, 2016.
- [27] V. Ramanishka, A. Das, D. H. Park, S. Venugopalan, L. A. Hendricks, M. Rohrbach, and K. Saenko. Multimodal video description. In A. Hanjalic, C. Snoek, M. Worring, D. C. A. Bulterman, B. Huet, A. Kelliher, Y. Kompatsiaris, and J. Li, editors, *Proceedings of the 2016 ACM Conference on Multimedia Conference, MM 2016, Amsterdam, The Netherlands, October 15-19, 2016*, pages 1092–1096. ACM, 2016.
- [28] A. Ranjan, J. Janai, A. Geiger, and M. J. Black. Attacking optical flow. In *2019 IEEE/CVF International Conference on Computer Vision, ICCV 2019, Seoul, Korea (South), October 27 - November 2, 2019*, pages 2404–2413. IEEE, 2019.
- [29] J. Redmon and A. Farhadi. Yolov3: An incremental improvement. *CoRR*, abs/1804.02767, 2018.
- [30] E. Riba, D. Mishkin, D. Ponsa, E. Rublee, and G. R. Bradski. Kornia: an open source differentiable computer vision library for pytorch. In *IEEE Winter Conference on Applications of Computer Vision, WACV 2020, Snowmass Village, CO, USA, March 1-5, 2020*, pages 3663–3672. IEEE, 2020.
- [31] V. D. Silva, J. Roche, and A. M. Kondoz. Robust fusion of lidar and wide-angle camera data for autonomous mobile robots. *Sensors*, 18(8):2730, 2018.
- [32] V. A. Sindagi, Y. Zhou, and O. Tuzel. Mvx-net: Multimodal voxelnet for 3d object detection. In *International Conference on Robotics and Automation, ICRA 2019, Montreal, QC, Canada, May 20-24, 2019*, pages 7276–7282. IEEE, 2019.
- [33] S. Thys, W. V. Ranst, and T. Goedemé. Fooling automated surveillance cameras: Adversarial patches to attack person detection. In *IEEE Conference on Computer Vision and Pattern Recognition Workshops, CVPR Workshops 2019, Long Beach, CA, USA, June 16-20, 2019*, pages 49–55. Computer Vision Foundation / IEEE, 2019.
- [34] J. Tu, M. Ren, S. Manivasagam, M. Liang, B. Yang, R. Du, F. Cheng,

- and R. Urtasun. Physically realizable adversarial examples for lidar object detection. *CoRR*, abs/2004.00543, 2020.
- [35] Y. Vorobeychik and M. Kantarcioglu. *Adversarial Machine Learning*. Morgan and Claypool, 2018.
 - [36] X. Wang, Y. Wang, and W. Y. Wang. Watch, listen, and describe: Globally and locally aligned cross-modal attentions for video captioning. In M. A. Walker, H. Ji, and A. Stent, editors, *Proceedings of the 2018 Conference of the North American Chapter of the Association for Computational Linguistics: Human Language Technologies, NAACL-HLT, New Orleans, Louisiana, USA, June 1-6, 2018, Volume 2 (Short Papers)*, pages 795–801. Association for Computational Linguistics, 2018.
 - [37] T. Wu, L. Tong, and Y. Vorobeychik. Defending against physically realizable attacks on image classification. In *International Conference on Learning Representations*, 2020.
 - [38] F. Wulff, B. Schäufele, O. Sawade, D. Becker, B. Henke, and I. Radusch. Early fusion of camera and lidar for robust road detection based on u-net FCN. In *2018 IEEE Intelligent Vehicles Symposium, IV 2018, Changshu, Suzhou, China, June 26-30, 2018*, pages 1426–1431. IEEE, 2018.
 - [39] C. Xiang, C. R. Qi, and B. Li. Generating 3d adversarial point clouds. In *IEEE Conference on Computer Vision and Pattern Recognition, CVPR 2019, Long Beach, CA, USA, June 16-20, 2019*, pages 9136–9144. Computer Vision Foundation / IEEE, 2019.
 - [40] B. Yang, M. Liang, and R. Urtasun. HDNET: exploiting HD maps for 3d object detection. In *2nd Annual Conference on Robot Learning, CoRL 2018, Zürich, Switzerland, 29-31 October 2018, Proceedings*, volume 87 of *Proceedings of Machine Learning Research*, pages 146–155. PMLR, 2018.
 - [41] Y. Yu, H. J. Lee, B. C. Kim, J. U. Kim, and Y. M. Ro. Investigating vulnerability to adversarial examples on multimodal data fusion in deep learning. *CoRR*, abs/2005.10987, 2020.
 - [42] W. Zhang, H. Zhou, S. Sun, Z. Wang, J. Shi, and C. C. Loy. Robust multi-modality multi-object tracking. In *2019 IEEE/CVF International Conference on Computer Vision, ICCV 2019, Seoul, Korea (South), October 27 - November 2, 2019*, pages 2365–2374. IEEE, 2019.